

Ab-initio spin dynamics applied to nanoparticles: canted magnetism of a finite Co chain along a Pt(111) surface step edge

B. Újfalussy¹, B. Lazarovits², L. Szunyogh^{2,3}, G. M. Stocks¹ and P. Weinberger²

¹Metals and Ceramics Division, Oak Ridge National Laboratory, Oak Ridge, Tennessee 37831, USA

²Center for Computational Materials Science, Technical University Vienna,
A-1060, Gumpendorferstr. 1.a., Vienna, Austria

³Department of Theoretical Physics and Center for Applied Mathematics and Computational Physics,
Budapest University of Technology and Economics, Budapest, Hungary

(Dated: Mar 25, 2004)

In order to search for the magnetic ground state of surface nanostructures we extended *first principles* adiabatic spin dynamics to the case of fully relativistic electron scattering. Our method relies on a constrained density functional theory whereby the evolution of the orientations of the spin-moments results from a semi-classical Landau-Lifshitz equation. This approach is applied to a study of the ground state of a finite Co chain placed along a step edge of a Pt(111) surface. As far as the ground state spin orientation is concerned we obtain excellent agreement with the experiment. Furthermore we observe noncollinearity of the atom-resolved spin and orbital moments. In terms of magnetic force theorem calculations we also demonstrate how a reduction of symmetry leads to the existence of canted magnetic states.

PACS numbers: 75.10.Lp, 75.30.Gw, 75.75.+a

Stimulated by the need for ever higher density recording media, atomic scale magnetic devices are presently at the very focus of experimental and theoretical research (see, e.g., the "viewpoint" drawn by Kübler [1]). Without doubt, understanding and design of the relevant physical properties – magnetic moments, magnetic anisotropy energies, thermal stability, switching – of atomic scaled magnets demand detailed knowledge of their electronic and magnetic structure. Several studies based on the Hubbard model [2, 3] or on density functional theory (DFT) [4, 5, 6, 7, 8] have attempted to explore the, mostly, noncollinear spin ground state of free and supported metallic clusters. While noncollinearity due to frustrated exchange interactions can be described in terms of a nonrelativistic theory [4, 5, 6, 7], general spin structures are subject to an interplay between the exchange and the spin-orbit interaction and, therefore, can only be studied within the framework of a relativistic electron theory [8].

An efficient tool to search for the equilibrium spin arrangement of a spontaneously magnetized system is to trace the time evolution of the spin moments until a stationary state is achieved. The foundations of the so-called first principles adiabatic spin-dynamics (SD) for itinerant electron systems were laid by Antropov *et al.* [9] in quite a general context. In short, for systems with well-defined local (atomic) moments, the evolution of the time dependent orientational configuration, $\{\mathbf{e}_i(t)\}$, is described by a microscopic, quasi-classical equation of motion,

$$\frac{d\mathbf{e}_i}{dt} = \gamma \mathbf{e}_i \times \mathbf{B}_i^{eff} + \lambda \left[\mathbf{e}_i \times (\mathbf{e}_i \times \mathbf{B}_i^{eff}) \right], \quad (1)$$

where \mathbf{B}_i^{eff} is an effective magnetic field averaged over the cell i , γ is the gyromagnetic ratio and λ is a damp-

ing (Gilbert) parameter. In this equation, the instantaneous orientational state is evaluated in terms of a self-consistent calculation within DFT. This formalism was further developed by Stocks *et al.* [10, 11] employing a constrained density functional theory[12]. Here a local (transverse) constraining field, \mathbf{B}_i^{con} – that can be determined selfconsistently – ensures the stability within DFT of the nonequilibrium orientational state demanded by the equation of motion. Clearly, the internal effective field that rotates the spins in the absence of a constraint and, therefore, has to be used in Eq. (1) is just the opposite of the constraining field [10]. By merging with the locally selfconsistent multiple scattering (LSMS) method SD has been applied to study the complex magnetic orderings in bulk metals and alloys [10, 11, 13].

In surface nanostructures, spin-orbit coupling – its importance magnified by the reduced, surface symmetry – obviously plays a key role in determining magnetic orientations. In order to deal with exchange splitting and relativistic scattering on an equal theoretical footing, we use the above first principles constrained DFT-SD scheme in conjunction with the Kohn-Sham-Dirac equation,

$$\begin{aligned} & [c \boldsymbol{\alpha} \cdot \mathbf{p} + \beta mc^2 + V(\mathbf{r}) \\ & + \mu_B \beta \boldsymbol{\sigma} \cdot (\mathbf{B}^{xc}(\mathbf{r}) + \mathbf{B}^{con}(\mathbf{r})) - E] \psi(\mathbf{r}) = 0. \end{aligned} \quad (2)$$

In this equation, $\boldsymbol{\alpha}$ and β are the usual Dirac matrices, $\boldsymbol{\sigma}$ are the Pauli matrices, $V(\mathbf{r})$ includes the Hartree and exchange-correlation potentials, while, within the local spin density approximation (LSDA), $\mathbf{B}^{xc}(\mathbf{r})$ is an exchange field interacting only with the spin of the electron. It should be noted that Eqs. (1) and (2) display the very basics of a relativistic *spin-only* dynamics, inasmuch no attempt is made to trace, distinctly, the time evolution of the orbital moments. Furthermore, although implied by

use of Eq. (2) with Eq. (1), we did not include a torque related to the coupling of the spin- and orbital degrees of freedom. As pointed out by Antropov *et al.* [9] this approach is only applicable when the deviation between the orientations of the spin and orbital moments is small.

In order to apply SD to nanostructures of finite size we have merged the above scheme with the multiple scattering theory (MST) Green's function embedded cluster method developed by Lazarovits *et al.* [14]. In this, a self-consistent calculation is first carried out for the surface system in terms of the relativistic Screened Korringa-Kohn-Rostoker method [15]. The nanostructure is subsequently *inserted* into this host using the conventional MST embedding formula,

$$\tau^c(\epsilon) = \tau^r(\epsilon) [\mathbf{I} - (\mathbf{t}^r(\epsilon)^{-1} - \mathbf{t}^c(\epsilon)^{-1}) \tau^r(\epsilon)]^{-1}. \quad (3)$$

In this equation, $\tau^r(\mathbf{t}^r)$ and $\tau^c(\mathbf{t}^c)$ are site-angular momentum matrices of the scattering path operators (single-site t -operators) of the host surface system and the cluster, respectively, and ϵ is the energy. By solving this equation together with the corresponding Poisson equation – with appropriate boundary conditions – a self-consistent calculation for the selected cluster can be performed that takes full account of the environment.

Recently, Gambardella *et al.* [16] reported the results of experiments on well characterized finite linear chains of Co atoms located at a step edge of a Pt(111) surface terrace. At 45 K the formation of ferromagnetic spin-blocks of about 15 atoms was observed with an easy magnetization axis normal to the chain and pointing along a direction of 43° towards the step edge. Previous DFT based studies related to this experiment calculated spin and orbital moments [17, 18, 19] and magnetic anisotropy energies of finite [18] and infinite [19] chains on Pt(111) surfaces using a magnetic force theorem (MFT) approach [20]. In what follows, we report the first attempt to obtain this canted magnetic state from first principles in a way that, simultaneously with the atomic potentials and effective fields, the directions of the magnetic moments are obtained selfconsistently.

We first performed a calculation for a Pt(111) surface in which 8 layers of Pt together with 4 layers of vacuum were treated selfconsistently. A seven-atom chain of Co together with 10 empty (vacuum) spheres were embedded into the topmost Pt layer as schematically indicated in Fig. 1 in order to create a nascent step edge and nested Co-chain. Simultaneously, all the nearest neighbors of the Co atoms were re-embedded into the respective Pt or vacuum layers to allow for relaxation of potentials around the Co chain. Thus, an effective embedded cluster of a total of 55 atoms was treated selfconsistently. Although the number of Co atoms we used in our model chain is substantially less than in the experiment, our previous experience in calculating magnetic properties of finite chains suggests that the local moments and the magnetic

anisotropy energy contributions of atoms in the interior of the chain quickly approach the corresponding values of an infinite chain [18].

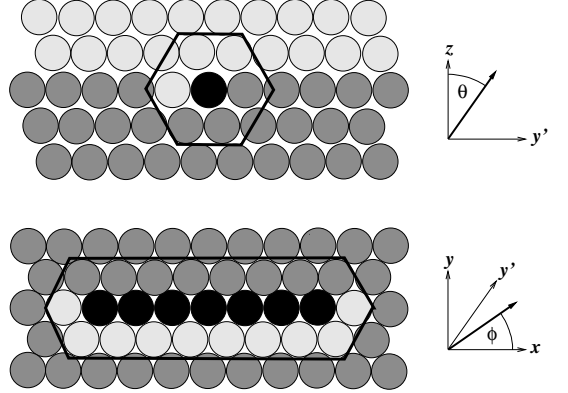


FIG. 1: Schematic view of the geometry of a seven-atom Co chain along a Pt(111) step edge. Full circles: Co atoms, shaded circles: Pt atoms, open circles: empty spheres. Top: side view, bottom: top view of the surface Pt layer with the Co chain. The embedded cluster is indicated by solid lines. The coordinate systems give reference to the azimuthal and polar angles, θ and ϕ , that characterize the orientation of the magnetization. (Note that in Ref. 16 a different coordinate system and the opposite notation for the angles is used.)

As mentioned before the present implementation of our SD scheme serves for searching the magnetic ground state of the system. From this point of view it is sufficient to consider only the second (damping) term on the right hand side of Eq. (1). The evolution of the spin orientation is then measured on a time scale with a unit (time step) of $1/\lambda$. A stable ground state is signaled by convergence of the θ and ϕ angles to a constant and concomitant convergence of the constraining fields to zero. In Fig. 2 the evolution of the θ and ϕ angles is plotted for the first 100 steps in this artificial time scale for each Co atom in the chain. Initially the directions of the atomic magnetic moments were set by a random number generator. It can be seen that after some oscillations both the θ and ϕ angles approach a very similar value for all the Co atoms. This means that the system rapidly tends to a nearly ferromagnetic order due to the strong ferromagnetic exchange coupling between the Co atoms. The initial rapid oscillations seen in Fig. 2 are the consequence of the relatively large constraining fields caused by the large exchange energies that result whenever the individual site moments point in very different directions. Once a nearly ferromagnetic configuration is achieved, the constraining fields drastically decrease, and a rather slow convergence of the orientations results. This slow convergence is due to the (much smaller) spin-orbit interaction energies and it takes about 1000 time steps for the ϕ and θ angles to converge. At this point the constraining fields are essentially zero, as is required for a ground state. The final converged state is characterized by a ϕ angle of 90°, i.e.,

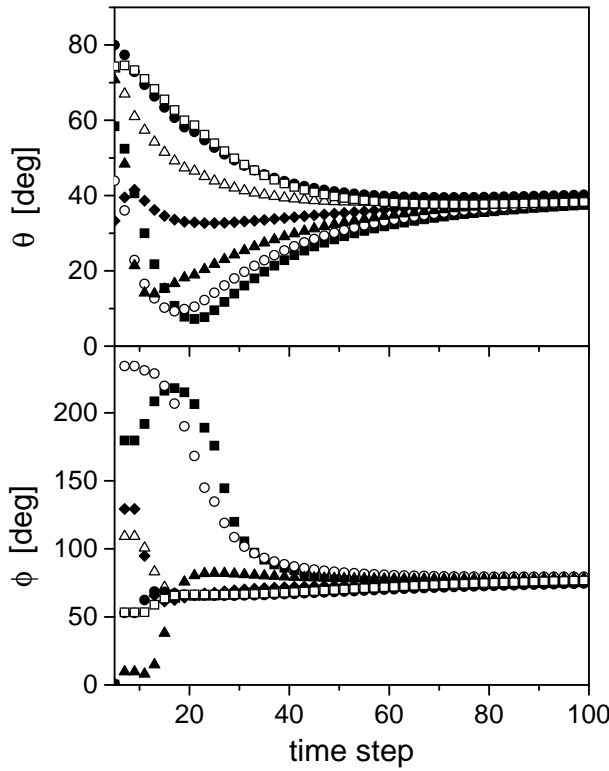


FIG. 2: Artificial time evolution of the angles θ (top) and the ϕ (bottom) angles defining the orientation of the spin moments for the seven Co atoms in the finite chain depicted in Fig. 1. The symbols refer to the following Co atoms numbered from the left to the right in the bottom part of Fig. 1: ■ 1, ○ 2, ▲ 3, ◆ 4, △ 5, ● 6, □ 7. Shown are the results for only the first 100 time steps. During the next 900 time steps the angles converge very smoothly

normal to the chain, with a spread of less than 1° , and θ angles of 42° . These results are in remarkable agreement with experiment [16], $\phi = 90^\circ$, $\theta = 43^\circ$. It is important to mention that the obtained ground state is apparently not induced by any symmetry of the system.

Once such a stable state has been established we can further analyze the resulting magnetic state in terms of the spin and orbital moments. For this purpose their size and the corresponding azimuthal angle θ for each Co atom are shown in Table I for each of the Co atoms in the chain. The first thing to notice is that the calculated spin moments for the inner Co atoms ($2.18 \mu_B$) are in good agreement with the value deduced from experiment ($2.12 \mu_B$) [16] and also with other theoretical studies on infinite wires [17, 19]. Atoms at both ends of the wire have larger spin (and orbital) moments than those within the wire similarly to our previous findings[18]. Although our calculated orbital moments for the inner atoms (0.19 – $0.20 \mu_B$) are somewhat larger than the corresponding values from other LSDA calculations ($0.16 \mu_B$ [17] and $0.15 \mu_B$ [19]), they are still much too small when compared to the experimental value ($0.68 \mu_B$) [16]. This aspect is a

well-known deficiency of the LSDA and often patched up using the so-called orbital polarization method or the LDA+U method.

atom	Spin moment		Orbital moment	
	moment(μ_B)	Θ (deg)	moment(μ_B)	Θ (deg)
1	2.23	41.1	0.25	39.1
2	2.18	42.5	0.20	41.5
3	2.18	42.3	0.19	40.1
4	2.18	42.4	0.20	41.3
5	2.18	42.3	0.19	40.2
6	2.18	42.5	0.20	41.5
7	2.23	41.1	0.25	39.1

TABLE I: Calculated magnitudes and orientations of the spin and orbital moments in a seven-atom Co chain along a Pt(111) step edge.

Another interesting feature of the magnetism of finite nanostructures is the noncollinearity of the moments. As can be seen from Table I the spin moments of the inner atoms are quite parallel while those at the end of the chain are misaligned by more than 1° . This can be traced to larger anisotropy energy contributions at chain end sites observed in finite chains earlier[18]. Most interestingly Table I also reveals differences of as much as 2° between the orientations of respective spin and orbital moments. This fact underlines the point made by Jansen [20], that within DFT the spin and orbital moments are aligned only when the ground state refers to a high-symmetry direction.

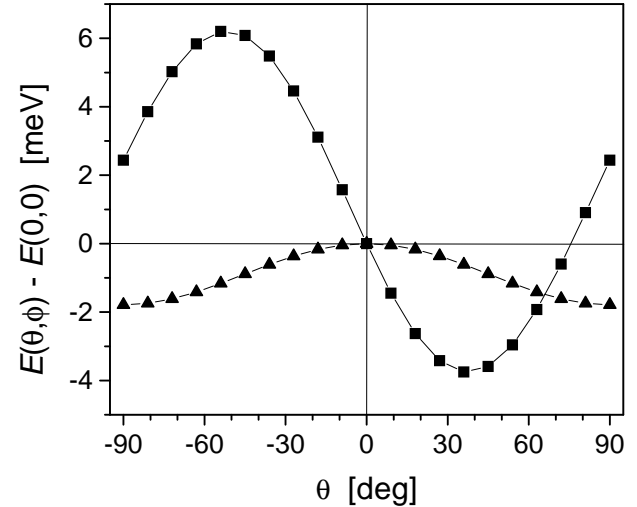


FIG. 3: Energy curves calculated using the magnetic force theorem for a ferromagnetic seven-atom Co wire at a Pt(111) surface step edge as a function of the azimuthal angle, θ . ■: $\phi = 90^\circ$, ▲: $\phi = 0^\circ$. Solid lines serve as a guide for eyes.

While it is necessary to perform fully selfconsistent calculations to obtain the details of the non-collinear ground

state, it is interesting to study this result in terms of the magnetic force theorem (MFT) [20]. Assuming ferromagnetic order great simplification can be achieved by calculating the energy of the system as a function of the orientation of a by then uniform magnetization, $E(\theta, \phi)$, such that the effective potentials and fields are kept fixed. Within this approach only the single particle (band) energy has to be taken into account. Fig. 3 shows the calculated curves of $E(\theta, \phi = 0^\circ)$ and $E(\theta, \phi = 90^\circ)$. In these calculations we used ground state selfconsistent potentials and fields obtained from the SD procedure. Clearly, the easy axis predicted by the MFT calculations, $\theta = 38^\circ$ and $\phi = 90^\circ$ is near the one obtained from the SD calculation. Furthermore, the hard axis is obtained at $\theta = -52^\circ$ and $\phi = 90^\circ$, i.e., by $\Delta\theta = -90^\circ$ away of the easy axis. This is again in good agreement with experiment [16].

For surfaces and interfaces with uniaxial symmetry the easy magnetization axis most often refers to either a normal or a parallel direction with respect to the planes. In case of a (y, z) mirror plane the energy of a ferromagnetic system can be written up to second order as

$$E(\theta, \phi) = E_0 + K_{2,1} \cos 2\theta + K_{2,2}(1 - \cos 2\theta) \cos 2\phi + K_{2,3} \sin 2\theta \sin \phi, \quad (4)$$

where $K_{2,i}$ ($i = 1, 2, 3$) are so-called anisotropy constants. Both calculated trajectories displayed in Fig. 3 coincide almost perfectly with the above function when using the parameters $K_{2,1} = -0.16$ meV, $K_{2,2} = -1.06$ meV, and $K_{2,3} = -4.81$ meV. It should be noted that, in terms of these anisotropy parameters, the easy axis corresponds to a direction, $\phi = \pi/2$ and

$$\theta = \frac{1}{2} \arctan \left(\frac{K_{2,3}}{K_{2,1} + K_{2,2}} \right). \quad (5)$$

The anisotropy energy as defined by the energy difference between the hard and the easy axes can also be read off Fig. 3: the corresponding value of 1.42 meV/Co atom compares favorably with the one deduced from the experiment (2.0 meV) [16]. It is worthwhile to mention, that in terms of similar MFT calculations Shick *et al.* obtained an easy axis along $\theta = 18^\circ$ and an anisotropy energy of 4.45 meV [19]. The difference of these values with respect to the present results can most possibly accounted for in the film geometry and/or the second-variational treatment of the spin-orbit coupling used in the FLAPW calculations of Ref.[19].

In this study we presented the first application of a relativistic ab initio spin dynamics as based on a constrained density functional theory to finite magnetic nanostructures. In excellent quantitative agreement with the corresponding experiment, we obtained a canted ground state for a Co wire along a Pt(111) surface step edge. We also found that this magnetic state is noncollinear: a feature that is expected to play a key role in nanostructures

having complex geometry. For the present relatively simple geometry the magnetic force theorem proved to be a useful tool to interpret the results of spin dynamics calculations and providing additional information such as anisotropy constants and the anisotropy energy.

Financial support was provided by the Center for Computational Materials Science (Contract No. GZ 45.451), the Austrian Science Foundation (Contract No. W004), and the Hungarian National Scientific Research Foundation (OTKA T038162 and OTKA T037856). The work of BU and GMS was supported by DOE-OS, BES-DMSE under contract number DE-AC05-00OR22725 with UT-Battelle LLC. Calculations were performed at ORNL-CCS (supported by OASCR-MICS) and NERSC (supported by BES-DMSE).

- [1] J. Kübler, *J. Phys.: Condens. Matter* **15**, V21 (2003)
- [2] M. A. Ojeda-López, J. Dorantes-Dávila, and G. M. Pastor, *J. Appl. Phys.* **81**, 4170 (1997).
- [3] S. Uzdin, V. Uzdin, and C. Demangeat, *Comp. Mat. Sci.* **17**, 441 (2000); *Surf. Sci.* **482-485**, 965 (2001).
- [4] T. Oda, A. Pasquarello, and R. Car, *Phys. Rev. Lett.* **80**, 3622 (1998)
- [5] O. Ivanov and V.P. Antropov, *J. Appl. Phys.* **85**, 4821 (1999).
- [6] D. Hobbs, G. Kresse, and J. Hafner, *Phys. Rev. B* **62**, 11556 (2000).
- [7] N. Fujima, *Eur. Phys. J. D* **16**, 185 (2001).
- [8] J. Anton, B. Fricke, and E. Engel, *Phys. Rev. A* **69**, 012505 (2004).
- [9] V. P. Antropov, M. I. Katsnelson, B. N. Harmon, M. van Schilfgaarde, and D. Kusnezov, *Phys. Rev. B* **54**, 1019 (1996).
- [10] G. M. Stocks, B. Újfalussy, Xindong Wang, D. M. C. Nicholson, W. A. Shelton, Yang Wang, A. Canning and B. L. Györfy, *Philos. Mag. B* **78**, 665 (1998).
- [11] B. Újfalussy, Xindong Wang, D. M. C. Nicholson, W. A. Shelton, G. M. Stocks, Yang Wang, and B. L. Györfy, *J. Appl. Phys.* **85**, 4824 (1999).
- [12] P. H. Dederichs, S. Blügel, R. Zeller and H. Akai, *Phys. Rev. Lett.* **53**, 2512, (1984).
- [13] G. M. Stocks, W. A. Shelton, T. C. Schulthess, B. Újfalussy, W. H. Butler, and A. Canning, *J. Appl. Phys.* **91**, 7355 (2002).
- [14] B. Lazarovits, L. Szunyogh, and P. Weinberger, *Phys. Rev. B* **65**, 104441 (2002).
- [15] L. Szunyogh, B. Újfalussy, and P. Weinberger, *Phys. Rev. B* **51**, 9552 (1995).
- [16] P. Gambardella, A. Dallmeyer, K. Maiti, M. C. Malagoli, W. Eberhardt, K. Kern, and C. Carbone, *Nature* **416**, 301 (2002); P. Gambardella, *J. Phys.: Condens. Matter* **15**, S2533 (2003).
- [17] M. Komelj, C. Ederer, J. W. Davenport, and M. Fähnle, *Phys. Rev. B* **66**, 140407 (2002).
- [18] B. Lazarovits, L. Szunyogh, P. Weinberger, *Phys. Rev. B* **67**, 024415 (2003).
- [19] A. B. Shick, F. Máca, and P. M. Oppeneer, [arXiv:cond-mat/0312467](https://arxiv.org/abs/cond-mat/0312467)

[20] H. J. Jansen, Phys. Rev. B **59**, 4699 (1999).